Nanotechnology Perceptions
ISSN 1660-6795
www.nano-ntp.com

CAViaR Greater Cane Rat Algorithm Enabled Deep learning for Autism Spectrum Disorder Classification Using Multi Model Data in Infant

Rakhee Kundu, Sunil Kumar

Computer Engineering, Amity University, Jaipur-Rajasthan, India
Email: sweetrakhee18@gmail.com

Autism Spectrum Disorder (ASD) involves brain enlargement in children, but its timing and implications are not fully understood. This complex disorder affects social interaction, behavior and communication. Although a cure remains elusive, early detection can improve quality of life. Current challenges in ASD detection include difficulties in early diagnosis due to subtle symptoms and inconsistencies in diagnostic criteria. This work develops an efficient model named; CAViaR Greater Cane Rate Algorithm enabled Deep Belief Network (CGCRA_DBN) for ASD detection using multimodal data. Initially, the images of the brain from the dataset are preprocessed using the Kuwahara filter and Region of Interest (ROI) extraction to eliminate noise and artifacts. The preprocessed images are then analyzed to identify pivotal regions based on functional connectivity, utilizing a box neighborhood search algorithm, thus generates the first output. Simultaneously, autism data is normalized using Z-score normalization. Following this, features are selected using the Hubert Index, and data augmentation is performed through bootstrapping, resulting in the second output. Both outputs are then utilized for classifying ASD with a Deep Belief Network (DBN) and the DBN is trained using the proposed CGCRA method, which integrates the Greater Cane Rat Algorithm (GCRA) with the Conditional Autoregressive Value at Risk (CAViaR) concept. Additionally, the system's performance is assessed using accuracy, specificity and sensitivity metrics, with the corresponding values obtained as 93.826%, 94.568% and 92.688%.

Keywords: Autism Spectrum Disorder, Deep Learning, Kuwahara Filter, Deep Belief Network, Greater Cane Rat Algorithm.

1. Introduction

The human cerebrum is a complex organ because the neuronic systems within it synchronize and form connections that can be organized into systems [9]. Brain disorders occur when parts of the brain fail to function properly, which can result problems with brain tissues and nerves. These disorders are often influenced by genetic factors, environmental risks, and other factors that affect specific regions of the nervous system. Common brain diseases include Autism, Brain Cancer, Alzheimer's disease, and various psychiatric disorders. ASD is a prevalent condition that impacts multiple areas of the brain, leading to neurological and developmental

challenges in children that can persist throughout their lives [6]. Autism affects multiple areas of the brain [5]. The World Health Organization (WHO) estimates that approximately 1 in 160 children around the world has ASD [7]. This condition presents a wide range of symptoms, including learning difficulties, behavioral challenges, atypical facial expressions, and poor eye contact [6]. To study brain disorders, Magnetic Resonance Imaging (MRI) is commonly employed. MRI provides detailed structural insights and high-resolution three-dimensional images of the brain [8]. Recently, the technique of multimodal fusion has gained significant attention in medical research and is increasingly used to enhance the diagnosis of ASD [14] [11].

Detecting autism is a demanding process that needs significant effort and time to manage effectively. While clinical and physiological features may not be identifiable early, certain key behavioral traits can be highly indicative of autism and its severity. Research has shown that eye movements are particularly useful as biomarkers for ASD, influencing responses to visual and verbal stimuli [13]. Although the exact causes of ASD remain unclear, some researchers believe that examining brain structure might offer valuable insights. Nevertheless, diagnosing ASD continues to be difficult due to its complex psychiatric symptoms and the limited availability of neurobiological evidence [10]. Multimodal data in ASD combines various information sources to improve understanding, diagnosis, and treatment of the disorder. Deep Learning (DL) is a type of machine learning method that automatically identifies key characteristics necessary for classification by analyzing data through multiple layers. Among Artificial Neural Networks (ANNs), Convolutional Neural Networks (CNNs) are crucial in computer vision, especially when applied to functional MRI (fMRI) data from individuals with ASD. The CNN approach can potentially identify brain biomarkers that are important for the early diagnosis and treatment of ASD [11]. In recent years, DL techniques have been widely used in medical and neurological fields, including, autism diagnosis, emotion recognition, patient-specific quality assurance, seizure detection and structural health monitoring [12].

The primary goal is to effectively detect ASD using a CGCRA-enabled DBN. This method first employs the Kuwahara Filter and ROI extraction for image preprocessing. The Box Neighborhood Search algorithm is then used for the extraction of pivotal region , resulting in the first output. On the other hand, the collected autism data is subsequently processed through normalization using Z-Score normalization, and crucial features are selected using Hubert Index. Data augmentation is accomplished using bootstrapping to generate the second output. Finally, ASD classification is done using the DBN, which is tuned using GCRA with the CAViaR concept.

The major highlight of this research is deliberated as follows.

- Proposed CGCRA-enabled DBN for ASD detection: An innovative method to detect ASD is designed employing CGCRA-enabled DBN. Here, classification is done using DBN and the hyperparameters are finely tuned by CGCRA.

The rest of the document is structured in the following way such that, Section 2 analyses traditional methods for detecting ASD, highlighting their advantages and limitations. Section 3 discusses the proposed method. Section 4 designates and analyzes the results of the proposed approach. Section 5 offers the conclusion.

2. Motivation

ASD diagnosis can be significantly improved with early detection to enhance developmental outcomes. Existing methods face challenges like symptom variability and subjective assessments, causing diagnostic delays. To address these issues and analyze complex patterns for better accuracy, a Deep Learning-based system is utilized to detect ASD.

2.1 Literature Survey

Kuttala, D., et al. [1] introduced a Dense Generative Adversarial Network (GAN) Architecture for ASD detection, which improved pattern detection by focusing on relevant features but it struggled with interpretation to new datasets. Sadiq, A., et al. [2] developed a Non-Oscillatory Connectivity (NOC) approach that reduced feature dimensions by highlighting key connections, but it failed to address specific brain areas or functions impacted by ASD. Li, G., et al. [3] presented a Landmark-based Multi-Instance Conv-Transformer (LD-MILCT) that reduced computational complexity and enhanced generalization, though it failed to incorporate additional information or consider physiological trait correlations. Neeharika, C.H. and Riyazuddin, Y.M., [4] devised a Multilayer Perceptron (MLP) classifier to lower diagnostic costs and detect high-risk cases early, but it required extensive data and validation to ensure generalizability across diverse clinical settings.

2.2 Major Challenges

The challenges encountered in the ASD detection process are outlined below:

- The DGAN approach in [1] improved detection accuracy for ASD but encountered difficulties in generalizing across different datasets and scanner setups, which potentially impacted its effectiveness in real-world applications.
- The NOC in [2] improved the classification of ASD subtypes by focusing on key brain connections, thereby enhancing diagnostic precision. However, it failed to examine the functional implications of specific brain areas and their variability among individuals.
- In [3], the LD-MILCT enhanced brain MRI classification for ASD by effectively reducing computational complexity but failed to include additional contextual information for correlations among physiological traits.
- The AI-based method [4] for ASD detection in children early diagnostic accuracy through advanced algorithms. However, it was limited by its dependence on extensive data and rigorous validation, which impacted its applicability and effectiveness.
- Detecting Autism Spectrum Disorder in infants is challenging, especially when using multi-modal data and current deep learning techniques. These challenges include managing the complexity of the data and ensuring accurate and timely predictions. Addressing these issues is essential for progressing early detection methods and enhancing intervention strategies.

3. Proposed CGCRA_DBN for ASD detection in Infants using Multi-modal data.

The chief intention of this paper is to design and develop a CGCRA trained DBN for ASD

detection utilizing brain images. Initially, the input brain image acquired from the database [23] undergoes preprocessing, where the Kuwahara filter [15] and ROI extraction [16] are applied to eliminate unwanted noise and artifacts. The preprocessed image is then used to extract pivotal regions derived from functional connectivity, employing the box neighborhood search algorithm. This phase yields the output-1. Simultaneously, autism data from a dataset [23] is processed through normalization using Z-score normalization [17]. Subsequently, feature selection is performed using the Hubert Index [18], and data augmentation is achieved through bootstrapping technique resulting the output-2. Both outputs are utilized for ASD classification with DBN [22], which is trained using the proposed CGCRA method integrating the GCRA) [21] with the CAVIaR concept [20]. Figure 1 illustrates the block diagram of the CGCRA_DBN approach for ASD detection using Multi-modal data.

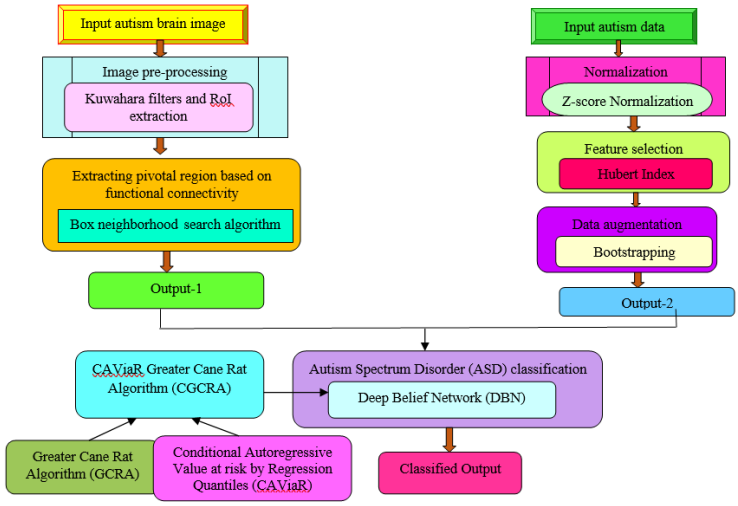

Figure 1. Block diagram of the proposed CGCRA_DBN for ASD detection

3.1 Acquisition of Input Image

Let us assume image database as E, which is represented as,

$$E = \{E_1, E_2, ...E_n .....E_j\} \quad (1)$$

where E specifies the brain image database, and E_n represents the n^{th} image from the total j samples.

3.2 Image Pre-processing based on Kuwahara Filter and RoI Extraction

Preprocessing is the method of transforming and organizing raw data to enhance its quality and suitability for accurate and efficient analysis. Here, the Kuwahara filter is encompassed to reduce noise and preserve edges, while ROI extraction isolates specific brain regions for accurate autism analysis. Here, the image E_n is used as the input for preprocessing.

3.2.1 Kuwahara Filter

Kuwahara Filter [15] enables more efficient noise reduction while preserving edges, preparing the image for segmentation and subsequent analysis operations. The filter window is divided into four regions, denoted as θ_n, where $n \in \{0,1,2,3\}$. For a filter in a square form with dimensions $(2\times m+1)\times(2\times m+1)$, each region θ_n contains $(m+1)\times(m+1)$ elements. In the specific case of a 3 × 3 filter window, each region will contain 4 elements. The variance α_n^2 of individual region is considered as,

$$\alpha_n^2 = \frac{1}{(m+1)\times(m+1)} \times \sum_{(p,q)\in\theta_n} [\beta(k(c,d)) - g_n]^2 \qquad (2)$$

where k represents the source image function, $k(c,d)$ denotes the value of the pixel at coordinates (c,d), β is a function that computes the value of a specific pixel and m is the value derived directly from the size of the filter window. The outcome from this phase is represented as R_n.

3.2.2 Extracting Regions of Interest (ROI)

The input for this segment is the filtered result R_n. ROI [16] extraction is crucial for diagnosing ASD using brain images. This step identifies the significant aspects of the image for subsequent analysis. The result obtained from this segment is referred to as S_n.

3.3 Extraction of Pivotal region employing Box Neighborhood Search algorithm

Extracting pivotal regions from brain images is crucial to identify the anatomical structures and lesions. The input provided to this stage is the preprocessed input S_n. The Box Neighborhood algorithm is employed to extract the pivotal region. First, partition the extracted RoI image into grid sections. Then, calculate the feature connectivity for each box using the expression given below.

$$P_n = \frac{PQ^b + \sum_{u=1}^{rb} PC_u^b + BD^{sb}}{f}, P = [0,1] \qquad (3)$$

where f signifies the normalizing factor, PQ^b signifies the Pearson correlation coefficient among pixels in the box, rb specifies the count of pixels in the b^{th} region, and BD^{sb} refers the feature derived from the normalized edge histogram.

Next, apply these steps to all the boxes present in the image. Finally, choose the boxes where the value of P is close to 1 and these are defined as the pivotal regions. The result obtained from this stage is signified as P_n.

3.4 Acquisition of Input data

Assess the database F containing autism data for detecting ASD, with the total data is expressed below,

$$F = \{F_1, F_2, ...F_n, ...F_j\} \qquad (4)$$

where, F indicates the database used for autism detection, and F_n refers the n^{th} data available from the entire j sample set.

3.4.1 Data Normalization utilizing Z-Score

Data normalization [17] involves transforming numerical data to a common range to reduce variability and improve data quality. This segment utilized the input autism data F_n with $[\partial \times \wp]$ which plots a values λ_e from the characteristic value H to G_n into a previously unknown range.

$$G_n = \frac{\lambda_e - H_e}{stdv(H)} \qquad (5)$$

where G_n denotes the outcome of normalization with $[\partial \times \wp]$, H_e indicates the mean of the attribute, and $stdv(H)$ refers to the attribute's standard deviation. The final result from this segment is uttered as.

3.4.2 Feature Selection using Hubert Index

The Hubert Index [18] quantifies the serial correlation coefficient among two matrices. For symmetric matrices, the input to this phase is G_n having dimension as $[\partial \times \wp]$.

$$V(\delta, v) = \frac{1}{Z_o} \sum_{\rho=1, \rho<\chi}^{\sigma=1} \delta_{\rho,\chi} V_{\rho,\chi} \qquad (6)$$

where, δ represents the proximity matrix and v defines the $\zeta \times \zeta$ matrix. The result from this phase is denoted as Y_n with dimension $[\partial \times \wp]$, such that $\partial > \wp$.

3.4.3 Data Augmentation using Bootstrapping Technique

Bootstrapping is a rapid and effective method for augmenting the data since it requires no enhanced data generation or analysis. It estimates the distribution of a statistic by resampling the data, helping to evaluate its variability and reliability. The input to this phase is Y_n with $[\partial \times \wp]$,and the result of this approach is called augmented data X_n, with dimensions $[\varpi \times \wp]$ such that $\partial > \varpi$.

3.5 ASD Classification using Proposed CGCRA_DBN

ASD involves a range of developmental conditions that impact communication, social

interaction, and behavioral patterns. Here, DBN is used to classify ASD, whose hyperparameters are tuned using proposed CGCRA. The input to this segment is signified as σ_n, such that $\sigma_n \in \{P_n, X_n\}$, here P_n denotes the output obtained by the Extraction of pivotal region whereas, X_n represents the Augmented data output.

3.5.1 Architecture of DBN

DBN [22] has become one of the most significant models in deep learning. It employs a generative model during the pretraining phase and utilizes backpropagation for fine-tuning. The RBM is often working as a layer-by-layer training model when building a DBN. It consists of a two-layer network that forms a specific kind of Markov random field, with "visible" units $r = \{0,1\}^A$ and "hidden" units $s = \{0,1\}^B$. The general architecture of DBN is represented in Figure 2.

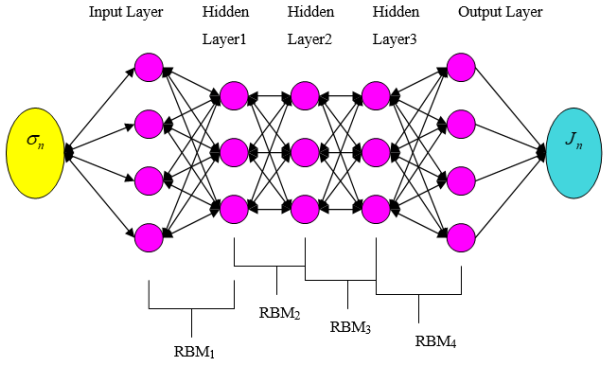

Figure 2. General Architecture of DBN

The energy of a joint configuration units is given by,

$$D(r,s,\lambda) = -\sum_{x=1}^{A} e_x r_x - \sum_{y=1}^{B} f_y s_y - \sum_{x=1}^{A}\sum_{y=1}^{B} h_x r_x s_y$$

$$= -e^K r - f^K s - r^K T s \qquad (7)$$

where, $\lambda = \{e_{x,} f_{y,} h_{xy}\}, h_{xy}$ represents the mass connecting visible unit x with hidden unit y ,while e_x and f_y are the bias terms for the visible and hidden units, correspondingly.

The joint distribution across the units is specified by,

$$J(r,s,\lambda) = \frac{1}{X(\lambda)} \exp(-D(r,s;\lambda)) \qquad (8)$$

$$X(\lambda) = \sum_{r}\sum_{s} D(r,s;\lambda) \qquad (9)$$

Here, $X(\lambda)$ is the constant value of normalization. The possibility of the training vector might be improved by modifying λ to decrease the energy, as shown in Eq. (7). The conditional distributions for the hidden unit s and the input vector r are represented by a logistic function.

$$l(s_y = 1 | r) = \vartheta\left(\sum_{x=1}^{A} T_{xy} r_x + e_y\right) \quad (10)$$

$$l(r_x = 1 | s) = \vartheta\left(\sum_{y=1}^{B} T_{xy} s_y + f_x\right) \quad (11)$$

$$\vartheta(v) = \frac{1}{1+\exp(-v)} \quad (12)$$

After the states of the hidden unit are established, the input data can be restored by assigning a value of 1 to each r_x based on the probability given in Eq. (11)

The learning of T is accomplished using a system recognized as Contrastive Divergence (CD). The adjustment to a weight is determined by,

$$\Omega T_{xy} = \in (r_x s_{y_{data}} - r_x s_{y_{reconstruction}}) \quad (13)$$

Here $\in$ signifies the learning rate and value of T is determined by the learning process. The output from this phase is denotes as J_n.

3.5.2 Hybrid Cavier GCRA Algorithm for Training

In ASD detection, the Caviar method and GCRA algorithm are employed to optimize model parameters and improve data distribution. The Caviar method optimizes parameter configurations to improve model accuracy, while GCRA enhances resource management and system performance. The hyperparameters are precisely tuned using Deep Belief Networks (DBNs) to ensure effective disease detection.

a) Solution Encoding

It is utilized to tackle optimization problems within a specified search space M to achieve the best possible solution, and it is outlined as,

$$M = [1 \times \eta] \quad (14)$$

Here, M denotes the search space, while η specifies the learning parameter of the DBN.

b) Fitness Function

Fitness functions play a critical role in optimization problems, as they guide the search for optimal solutions. They are represented as,

$$W = \frac{1}{j}\sum_{n=1}^{j}\left[IN - J_n\right]^2 \qquad (15)$$

Here, the targeted output is IN and J_n represents the output attained from DBN classifier.

c) Algorithmic Steps

The algorithmic stages involved in this method are outlined below.

Step 1: Initialize the Population

The GCRA optimization process initiates by the random creation of a Greater Cane Rats (GCR) population (W) and this process involves utilizing the Upper Bound (UB) and Lower Bound (LB).

$$O = \begin{bmatrix} o_{1,1} & o_{1,2} & \cdots & o_{1,a-1} & o_{1,a} \\ o_{2,1} & o_{2,2} & \cdots & o_{2,a-1} & o_{2,a} \\ \vdots & \vdots & o_{wz} & \vdots & \vdots \\ o_{h,1} & o_{h,2} & \cdots & o_{h,a-1} & o_{h,a} \end{bmatrix} \qquad (16)$$

Here, O denotes the complete GCR population, with each individual rat O_{wz} positioned in the z^{th} dimension, while h and a refers to the population size and problem dimension.

Step 2: Evaluate the Fitness Function

The fitness function is tuned continuously until an optimal solution is achieved which is done using Eq. (15).

Step 3: Update GCR

In the GCRA framework, the dominant rat is termed as the fittest, and its position vector provides the optimal value for the objective function, which is denoted as O_{dom}. The GCRA alternates between exploration and exploitation phases based on a variable χ that reflects the rainy season. The value of χ, which is crucial for balancing exploration and exploitation, is meticulously adjusted to 0.5 following extensive parametric analysis.

$$o_{w,z}^{new} = 0.7 * \frac{(o_{w,z} + o_{dom,z})}{2} \qquad (17)$$

Here, $o_{w,z}^{new}$ represents the location of the new GCR, $o_{w,z}$ locates the current GCR, $o_{dom,z}$ is the male dominant in the z^{th} dimension.

Step 4: Exploration Phase

A new location for the leftover rats in the search space is established based on the position of the dominant male, as outlined in the given equation,

$$o_{w,z}^{new} = o_{w,z} + N \times (o_{dom,z} - fs \times o_{w,z}) \quad (18)$$

Here, N is a random numeral that is well-defined within the boundaries of the problem space, representing distributed food sources and accommodation, while fs simulates the impact of an enormous food source.

Step 5: Exploitation Phase

This phase is initiated by arbitrarily choosing a female fe, with the condition that, $fe \neq o_{dom}$. Since breeding occurs in areas with plentiful food, the focus of activity intensifies around the selected female. This process is described by Eq. (19) $o_{w,z}^{new} = o_{w,z} + N \times (o_{dom,z} - \tau \times o_{fe,z})$ (19)

Let us consider, $o_{w,z}^{new} = o_{w,z}^{t+1}$ (20)

$$o_{w,z} = o_{w,z}^{t} \quad (21)$$

$$o_{dom,z} = o_{dom,z}^{t} \quad (22)$$

$$o_{fe,z} = o_{fe,z}^{t} \quad (23)$$

Substituting the above equations in Eq. (19)

$$o_{w,z}^{t+1} = o_{w,z}^{t} + N \times (o_{dom,z}^{t} - \tau \times o_{fe,z}^{t}) \quad (24)$$

By applying the Caviar concept, the above equation becomes

$$o_{w,z}^{t} = \alpha_0 + \sum_{ab=1}^{cd} \alpha_{ab} * o_{w,z}^{t-ab} + \sum_{ab=1}^{ef} \alpha_n \, fx(o_{w,z}^{t-no}) \quad (25)$$

$$o_{w,z}^{t} = \alpha_0 + \alpha_1 o_{w,z}^{t-1} + \alpha_2 o_{w,z}^{t-2} + \alpha_1 \, fx(o_{w,z}^{t-1}) + \alpha_2 \, fx(o_{w,z}^{t-2}) \quad (26)$$

Substituting Eq. (26) in Eq. (24), The update solution of CGCRA is as follows,

$$o_{w,z}^{t+1} = \alpha_0 + \alpha_1 o_{w,z}^{t+1} + \alpha_2 o_{w,z}^{t-2} + \alpha_1 \, fx(o_{w,z}^{t-1}) + \alpha_2 \, fx(o_{w,z}^{t-2}) + N \times (o_{dom,z}^{t} - \tau \times o_{fe,z}^{t}) \quad (27)$$

Here, τ selects a value from 1 to 4 in an arbitrary manner, $o_{fe,z}$ denotes the location of the arbitrarily chosen female in the z^{th} position, N and τ are pivotal for optimizing exploration and exploitation all over the iterations.

Step 6: Update Search Agent

In the concluding stage of the exploration phase, the GCR will move to the newly computed position only if it improves the neutral function value; otherwise, it will remain in its current position and the migration plan is withdrawn using the below equation as,

$$O_w = \begin{cases} o_{w,z} + N \times (o_{w,z} - \Im \times o_{fe,z}), F_w^{new} < F_w \\ o_{w,z} + N \times (o_{dom,z} - \Re \times o_{fe,z}), otherwise \end{cases} \quad (28)$$

Here, O_w denotes the new or forthcoming state of the w^{th} GCR, F_w is the current objective function value for the GCR. $\Im$ is a coefficient representing the diminishing availability of food, which initiates the exploration for alternative food and shelter options. Meanwhile, $\Re$ is the constant that encourages the GCR to relocate to other sources for plenty of food.

Step 7: Reevaluate the Fitness Function

The fitness is repeatedly assessed to minimize error and identify the optimal solution.

Step 8: Termination

This process is repeated until an optimal solution is achieved, with iterative adjustments made throughout the process.

4. Results and Discussion

The following section provides a detailed explanation of the results and discussions for the developed CGCRA_DBN.

4.1 Experimental Setup

CGCRA_DBN is developed for detecting ASD using brain images and autism data, and it is implemented using the Python tool.

4.2 Experimental Outcomes

The results of CGCRA_DBN are detailed in Figure 3. 3 a) displays the input Image-1, while 3 b) presents the input Image-2. The preprocessing Image-2 is shown in Figure 3 c), with the processed Image-2 depicted in Figure 3 d). Figure 3 e) illustrates RoI Image-1, and Figure 3 f) demonstrates RoI Image-2.

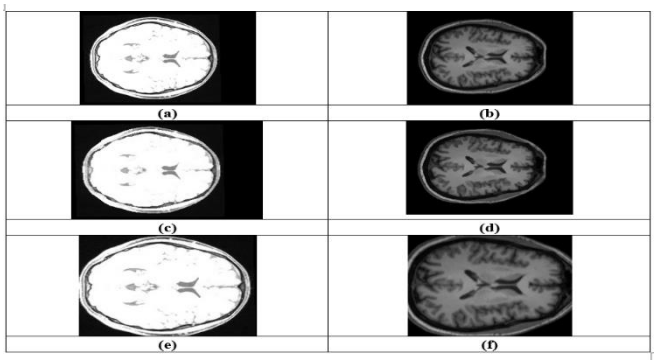

Figure 3. Experimental results of CGCRA_DBN, a) Input image -1, b) Input image -2, c) Preprocessed image -1, d) Preprocessed image -2 e) RoI image -1 e), f) RoI image -2

4.3 Dataset Description

The ACERTA ABIDE dataset [23] is used in ASD detection to provide a comprehensive set of neuroimaging and behavioral data for analyzing brain connectivity patterns. This helps in identifying distinctive features and biomarkers associated with Autism Spectrum Disorder.

4.4 Performance Metrics

The metrics used to evaluate ASD are accuracy, specificity, and sensitivity.

4.4.1 Accuracy: Accuracy [19] of the classification model reflects its overall performance and can be calculated using the formula provided below.

$$Accuracy = \frac{A_{bc} + A_{nc}}{A_{bc} + A_{nc} + D_{ec} + D_{fc}} * 100 \quad (29)$$

Here, A_{bc} indicates true positives, A_{nc} denotes false positives, D_{ec} represents true negatives, and D_{fc} states false negatives.

4.4.2 Specificity: Specificity [19] measures the non-affected ASD people among the total number of cases and it is calculated using the formula stated below.

$$Specificity = \frac{A_{nc}}{A_{nc} + D_{ec}} * 100 \quad (30)$$

4.4.3 Sensitivity: Sensitivity [19] is the ratio of detecting ASD affected people among the total number of cases and the formula for calculating sensitivity is as follows,

$$Sensitivity = \frac{A_{bc}}{A_{bc} + D_{fc}} * 100 \quad (31)$$

4.5 Comparative Techniques

To evaluate the performance of the CGCRA_DBN, it is compared with traditional ASD detection methods, including the Dense Attentive GAN [1], NOC [2], LD-MILCT [3], MLP classifier [4], and GAOOBO_CNN_TL.

4.6 Comparative Assessment

The comparative assessment of CGCRA_DBN based on ASD detection utilizing the ABIDE database [23], is done by varying the training data from 50% to 90%.

4.6.1 Assessment based on CGRA_DBN utilizing ABIDE I

Figure 4 illustrates the comparative assessment of CGCRA_DBN for ASD detection with 90% training data. Figure 4 a) shows the assessment of CGCRA_DBN regarding accuracy CGCRA_DBN achieves an accuracy of 93.699%, that surpasses conventional methods that achieves the accuracies of 86.817%, 87.169%, 88.560%, 89.490%, and 91.143%. Here, performance improvement of proposed over these models is 7.344%, 6.969%, 5.485%, 4.492%, and 2.728%, respectively. Figure 4 b) shows the estimation of proposed approach in

relation to Specificity. The specificity gained by CGCRA_DBN's is 94.263%, whereas the prior models attained the specificity as 87.112%, 88.440%, 89.742%, 90.116% and 91.945%. However, the designed model CGCRA_DBN's outperforms by 7.587%, 6.177%, 4.796%, 4.400%, and 2.459%, respectively. Figure 4 c) determines the estimation of CGCRA_DBN method with respect to sensitivity. The CGCRA_DBN's attained the sensitivity as 92.329%, while traditional methods achieved sensitivity of 85.838%, 86.251%, 87.494%, 88.967%, and 89.874%. Here, the performance gain attained by the designed model over conventional techniques are 7.030%, 6.582%, 5.236%, 3.641%, and 2.659%, respectively.

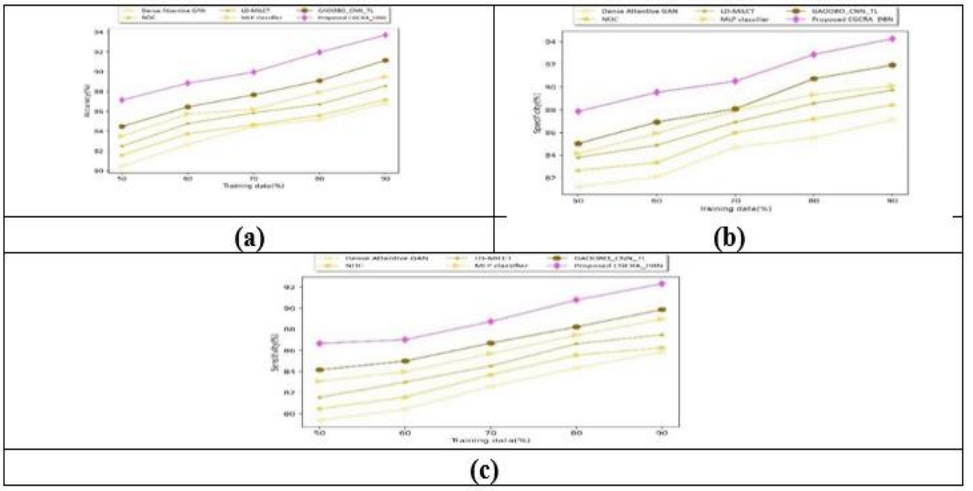

Figure 4. Assessment of CGCRA_DBN utilizing ABIDE I, a) accuracy b) specificity c) sensitivity

4.6.2 Assessment based on CGRA_DBN utilizing ABIDE II

Figure 5 presents a comparative evaluation of CGCRA_DBN for ASD detection by altering training data. Figure 5 a) represents the assessment of CGCRA_DBN with respect to accuracy. CGCRA_DBN achieved an accuracy of 93.826%, whereas the conventional methods attained the accuracy of 86.214%, 87.569%, 88.583%, 89.760%, and 91.707%. However, the designed approach outperforms the classical models by 8.112%, 6.669%, 5.588%, 4.333%, and 2.258%, respectively. Figure 5 b) demonstrates the estimation of the proposed approach with respect to specificity. The specificity attained by CGCRA_DBN is 94.568%, while the previous methods gained the specificity as 87.109%, 88.147%, 89.959%, 90.687%, and 92.058%. CGCRA_DBN performance gain exceeds these methods by 7.887%, 6.789%, 4.873%, 4.103%, and 2.654%, respectively. Figure 5 c) illustrates the estimation of the CGCRA_DBN method with regard to sensitivity and the proposed model gained the sensitivity as 92.688%, whereas traditional methods has obtained the sensitivity of 85.214%, 86.978%, 87.932%, 88.317%, and 90.644%. The novel CGCRA_DBN surpasses other conventional techniques by 8.062%, 6.160%, 5.131%, 4.715%, and 2.204%.

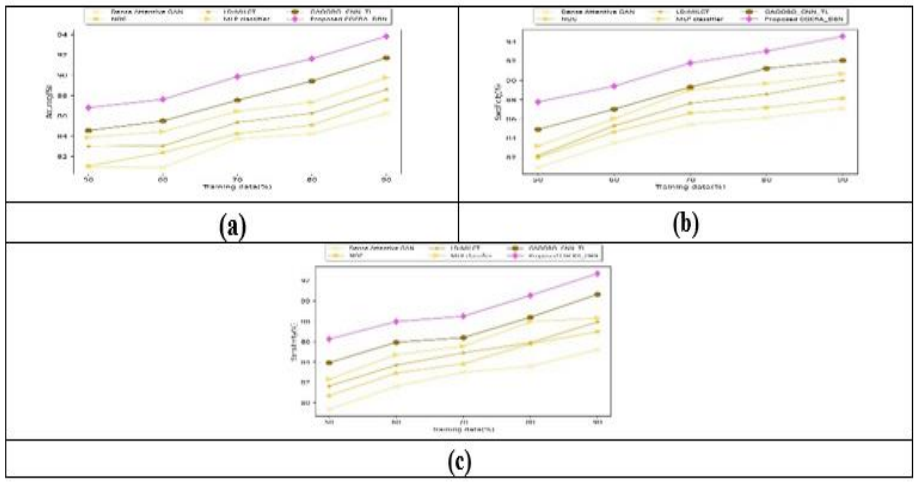

Figure 5. Assessment of CGCRA_DBN using ABIDE II, a) accuracy b) specificity c) sensitivity

4.7 Comparative Discussion

Table 1 shows the comparative discussion of various methods and shows that CGCRA_DBN performs better than Dense Attentive GAN, NOC, LD-MILCT, MLP classifier, and GAOOBO_CNN_TL when using the ABIDE II database with adjusted training data. The other methods achieved accuracies of 86.214%, 87.569%, 88.583%, 89.760%, and 91.707%, while CGCRA_DBN achieved an accuracy of 93.826%. This higher accuracy indicates that CGCRA_DBN has fewer false positives and fewer misdiagnoses. Additionally, CGCRA_DBN achieved a specificity of 94.568%, which is higher than the 87.109%, 88.147%, 89.959%, 90.687%, and 92.058% seen in the other methods. This shows that CGCRA_DBN is more effective at identifying the distinct features of autism spectrum disorder (ASD). In terms of sensitivity, CGCRA_DBN reached 92.688%, exceeding the 85.214%, 86.978%, 87.932%, 88.317%, and 90.644% achieved by the other methods. This improvement reduces the risk of misdiagnosing ASD and missing comorbid mental health conditions commonly associated with it. Overall, CGCRA_DBN is shown to be a highly effective method for detecting ASD.

Data set	Analysis based on	Metrics/ Methods	Dense Attentive GAN	NOC	LD-MILCT	MLP classifier	GAOOBO_CNN_TL	Proposed CGCRA_DBN
ABIDE I	***Training data= 90%***	*Accuracy (%)*	86.817%,	87.169%	88.560%	89.490%	91.143%	93.699%
		Specificity (%)	87.112%	88.440%	89.742%	90.116%	91.945%	94.263%
		Sensitivity (%)	85.838%	86.251%	87.494%	88.967%	89.874%	92.329%
ABIDE II	***Training data= 90%***	*Accuracy (%)*	86.214%	87.569%	88.583%	89.760%	91.707%	**93.826%**
		Specificity (%)	87.109%	88.147%	89.959%	90.687%	92.058%	**94.568%**
		Sensitivity (%)	85.214%	86.978%	87.932%	88.317%	90.644%	**92.688%**

Table 1. Comparative discussion of CGCRA_DBN

5. Conclusion

Autism Spectrum Disorder is characterized by difficulties with social interaction, behavioral issues, and communication challenges. Early diagnosis is challenging due to subtle symptoms and inconsistent diagnostic criteria. Although there is no cure, early intervention is crucial for improving quality of life. This work enhances ASD detection effectively by utilizing the CGCRA_DBN approach with multimodal data. Brain images are preprocessed with Kuwahara filter, and ROI extraction is used to remove noise and artifacts. The pivotal region is extracted using the box neighborhood search algorithm, resulting the first output. On the other hand, Autism data is normalized with Z-score normalization, and feature selection is performed using the Hubert Index. Thereafter, data augmentation is achieved through bootstrapping technique, resulting the second output. These outputs are fused together to classify the ASD using DBN, which is trained by CGCRA and it is developed by the integration of CAViaR concept with GCRA. The system's effectiveness is evaluated using accuracy, specificity and sensitivity metrics, 93.826%, 94.568% and 92.688% showing significant advancements in ASD detection and classification. Future study in ASD classification should aim to improve accuracy using advanced algorithms, with large datasets and enhancing model interpretability for clinical application.

References

[1] Kuttala, D., Mahapatra, D., Subramanian, R. and Oruganti, V.R.M., "Dense attentive GAN-based one-class model for detection of autism and ADHD", Journal of King Saud University-Computer and Information Sciences, vol. 34, no. 10, pp.10444-10458, 2022.

[2] Sadiq, A., Al-Hiyali, M.I., Yahya, N., Tang, T.B. and Khan, D.M., "Non-oscillatory connectivity approach for classification of autism spectrum disorder subtypes using resting-state fMRI", IEEE Access, vol. 10, pp.14049-14061, 2022.

[3] Li, G., Ji, Z. and Sun, Q., "Deep Multi-Instance Conv-Transformer Frameworks for Landmark-Based Brain MRI Classification", Electronics, vol. 13, no. 5, pp. 980, 2024.

[4] Neeharika, C.H. and Riyazuddin, Y.M., "Developing an Artificial Intelligence Based Model for Autism Spectrum Disorder Detection in Children", Journal of Advanced Research in Applied Sciences and Engineering Technology, vol. 32, no. 1, pp. 57-72, 2023.

[5] Khodatars, M., Shoeibi, A., Sadeghi, D., Ghaasemi, N., Jafari, M., Moridian, P., Khadem, A., Alizadehsani, R., Zare, A., Kong, Y. and Khosravi, A., "Deep learning for neuroimaging-based diagnosis and rehabilitation of autism spectrum disorder: a review", Computers in biology and medicine, vol. 139, pp.104949, 2021.

[6] Ashraf, A., Zhao, Q., Bangyal, W.H. and Iqbal, M., "Analysis of brain imaging data for the detection of early age autism spectrum disorder using transfer learning approaches for Internet of Things" IEEE Transactions on Consumer Electronics, 2023.

[7] Subah, F.Z., Deb, K., Dhar, P.K. and Koshiba, T., "A deep learning approach to predict autism spectrum disorder using multisite resting-state fMRI", Applied Sciences, vol. 11, no, 8, pp.3636, 2021.

[8] Jain, S., Tripathy, H.K., Mallik, S., Qin, H., Shaalan, Y. and Shaalan, K., "Autism Detection of MRI Brain Images Using Hybrid Deep CNN With DM-Resnet Classifier", IEEE Access, 2023.

[9] Saleh, A.Y. and Chern, L.H.,"Autism Spectrum Disorder Classification Using Deep Learning", International Journal of Online & Biomedical Engineering, vol. 17, no, 8, 2021.

[10] Ke, F., Choi, S., Kang, Y.H., Cheon, K.A. and Lee, S.W., "Exploring the structural and strategic bases of autism spectrum disorders with deep learning", Ieee Access, vol. 8, pp.153341-153352,

2020.
[11] Ganesh, K., Umapathy, S. and Thanaraj Krishnan, P., "Deep learning techniques for automated detection of autism spectrum disorder based on thermal imaging", Proceedings of the Institution of Mechanical Engineers, Part H: Journal of Engineering in Medicine, vol. 235, no, 10, pp.1113-1127, 2021.
[12] Nogay, H.S. and Adeli, H., "Multiple classification of brain MRI autism spectrum disorder by age and gender using deep learning" Journal of Medical Systems, vol. 48, no, 1, pp.15, 2024.
[13] Ahmed, I.A., Senan, E.M., Rassem, T.H., Ali, M.A., Shatnawi, H.S.A., Alwazer, S.M. and Alshahrani, M., "Eye tracking-based diagnosis and early detection of autism spectrum disorder using machine learning and deep learning techniques" Electronics, vol. 11, no, 4, pp.530, 2022.
[14] Han, J., Jiang, G., Ouyang, G. and Li, X., "A multimodal approach for identifying autism spectrum disorders in children" IEEE Transactions on Neural Systems and Rehabilitation Engineering, vol. 30, pp.2003-2011, 2022.
[15] Bartyzel, K., "Adaptive kuwahara filter", Signal, image and video processing, vol.10, pp.663-670, 2016.
[16] Rossi, L., Karimi, A. and Prati, A., "A novel region of interest extraction layer for instance segmentation" In 2020 25th international conference on pattern recognition (ICPR), pp. 2203-2209, IEEE, January 2021.
[17] Prihanditya, H.A., "The implementation of z-score normalization and boosting techniques to increase accuracy of c4. 5 algorithm in diagnosing chronic kidney disease", Journal of Soft Computing Exploration, vol. 1, no, 1, pp.63-69, 2020.
[18] Gustriansyah, R., Suhandi, N. and Antony, F., "Clustering optimization in RFM analysis based on k-means", Indonesian Journal of Electrical Engineering and Computer Science, vol. 18, no, 1, pp.470-477, 2020.
[19] Muhammad, Y., Tahir, M., Hayat, M. and Chong, K.T., "Early and accurate detection and diagnosis of heart disease using intelligent computational model" Scientific reports, vol. 10, no, 1, pp.19747, 2020.
[20] Engle, R.F. and Manganelli, S., "CAViaR: Conditional autoregressive value at risk by regression quantiles", Journal of business & economic statistics, vol. 22, no, 4, pp.367-381, 2004.
[21] Agushaka, J.O., Ezugwu, A.E., Saha, A.K., Pal, J., Abualigah, L. and Mirjalili, S., "Greater cane rat algorithm (GCRA): A nature-inspired metaheuristic for optimization problems", Heliyon, 2024.
[22] Chen, Y., Zhao, X. and Jia, X., Spectral–spatial classification of hyperspectral data based on deep belief network. IEEE journal of selected topics in applied earth observations and remote sensing, vol. 8, no, 6, pp.2381-2392, 2015.
[23] The acerta-abide database will be taken from "https://github.com/lsa-pucrs/acerta-abide" accessed on August, 2024.